Design and test of an X-band optimal rain rate estimator in the frame of the RHYTMME Project

Fadela Kabeche, Jordi Figueras i Ventura, Béatrice Fradon, Abdel-Amin Boumahmoud, Stephen Frasier, Pierre Tabary
Météo France, 42 Av Coriolis, 31057 Toulouse CEDEX, France,fadela.kabeche@meteo.fr
(Dated: 30 May 2012)

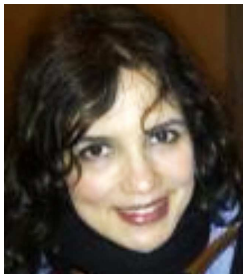

Fadela Kabeche

1. Introduction

The RHYTMME project (Risques HYdro-météorologiques en Territoires de Montagnes et MEditerranéens) was developed in order to establish a platform of services allowing a better management of hydrometeorological risks in the French southern Alps, which are prone to intense precipitation events and flash floods. In the frame of the RHYTMME Project, Météo France is deploying a dense network of 4 polarimetric X-band radars over the period 2010 – 2013. The first radar (Mont Maurel) is installed and operating since May 2010. The data from another radar (Mont Vial), owned by CNRS and operated by Novimet, is also used. The objective is to generate high-quality networked products, including quantitative precipitation estimation (QPE) mosaics, appropriate for integration into automatic hydrometeorological alerting systems.

Radar QPE in a mountainous environment is rather challenging due to issues such as occultation, partial beam blocking (PBB), partial beam filling, etc. Moreover, although X-band radars have the advantage of smaller sensitivity to ground clutter and reduced size and cost, they also suffer from much more attenuation than radar at longer wavelengths. This paper investigates the optimal QPE algorithm to operate in such an environment. Several polarimetric QPE algorithms have been tested such as K_{DP} -based algorithms, conventional Z-R algorithms (with and without attenuation correction), and Testud et al. (2000) ZPHI®. The differential reflectivity (Z_{DR}) has not been used in the tests because its current stability and accuracy is considered insufficient. In a first stage, only single tilt data has been used in order to simplify the evaluation.

Section 2 of this paper describes the operational RHYTMME radar data processing chain. Section 3 describes the evaluation methodology followed. Section 4 discusses the results. The sensitivity of the Φ_{DP} filtering and the K_{DP} estimation have been thoroughly evaluated as well as the impact of the attenuation correction. Finally, conclusions are drawn in section 5.

2. The RHYTMME radar data processing chain

A dedicated radar data processing chain was developed in the framework of the project and has been operational since fall 2011. This chain has the novelty that raw radar data is concentrated in the Météo France center in Toulouse where the final radar products are generated instead of being generated by each individual radar. The raw radar data (moments) are stored on a server and are available for off-line processing. This new architecture can be considered the prototype for future radar data processing at Météo France. The polarimetric radar processing chain has been adapted from an S- and C-band in-house developed chain which is described in detail in Boumahmoud et al. (2010).

The polarimetric variables collected by the X band radars are Z_H, Z_{DR}, Φ_{DP} and co-polar correlation coefficient (ρ_{HV}) in polar coordinates. The range resolution is 300 m for Mont Vial and oversampled to 240 m for Mont Maurel, while the azimuthal resolution is oversampled to 0.5° for both radars. Mont Maurel radar also provides the standard deviation of the reflectivity from pulse to pulse (σ_Z) at 1 km^2 resolution. In addition, both radars provide mean Doppler velocity (v_D) and Doppler spectral width (σ_v).

Since the radars in the network are heterogeneous, the first step in the processing is, if necessary, a pre-treatment of the data to put it in a uniform format that can be ingested into the polarimetric processing chain. The second step is the processing of the raw X-band polarimetric variables. The inputs of the this chain are the polarimetric fields of Z_H, Z_{DR}, Φ_{DP}, ρ_{HV} in polar coordinates and a Cartesian field of σ_Z. The chain performs successively the following operations: calibration of Z_H and Z_{DR}, PBB correction using static propagation maps, non-meteorological echo identification, ρ_{HV}-based bright band identification, Φ_{DP} offset removal and filtering, K_{DP} estimation, attenuation correction, hydrometeor classification and the computation of daily monitoring indicators (Bias curves for Z_H and Z_{DR}, offset curves for Φ_{DP}, average ρ_{HV} in rain, etc.)

Since the echo type classification and the attenuation correction are strongly dependent upon the radar frequency, these modules have been adapted to X-band. It is important to notice that these modules are all linked. For example, misidentified clutter echoes can lead to aberrant values of the precipitation field for an entire ray due to the resultant wrong attenuation correction. On the other hand, the identification of precipitation as clutter leads to gaps in the rain field, which is a serious issue in areas that already suffer heavily from clutter.

The outputs of the polarimetric chain are Z_{DR} and Z_H (with and without attenuation correction), ρ_{HV}, Φ_{DP} corrected from offset and filtered (using a running median filter of 25 gates), estimated K_{DP}, texture of Z_{DR}, the estimated path-integrated attenuation and differential attenuation, σ_Z and the echo type classification in polar coordinates. The corrected Z_H, the echo

type and the Path Integrated Attenuation (PIA) are also provided, in Cartesian coordinates.

The next step is to combine the processed polarimetric information available on PPIs to generate the best surface estimation of the 1 km², 5' rainfall accumulation using a polarimetric QPE algorithm. Finally, mosaic images are constructed using both RHYTMME radars and the nearest radars of the Météo France network.

3. The QPE processing chain

A polarimetric QPE processing chain, designed for evaluation purposes, that obtains hourly precipitation accumulation estimation from single tilts has been implemented (Figueras i Ventura et al., 2012). The inputs of the algorithm evaluation are the outputs of the polarimetric pre-processing chain. The first step is to estimate the instantaneous rainfall rate in areas classified as precipitation (PR) by the polarimetric chain using one of the tested algorithms.

The outputs of the algorithms are then converted from polar to Cartesian coordinates using a Cressman Analysis. At this point the data is re-evaluated according to the echo type. Pixels classified as noise, single polarization (low SNR), sea clutter and clear air are re-assigned from missing value to 0 mm/h rainfall rate. To compensate for the advection between measurements interpolation is performed using an advection field calculated a priori from the evolution of the previous reflectivity measurements. The interpolated rainfall rate field is integrated in time to obtain the 5' precipitation accumulation. The addition of twelve 5'precipitation accumulation fields then yield the hourly rainfall accumulation.

The hourly rainfall accumulation is compared to the hourly rainfall accumulation obtained by the high density network of rain gauges operated by Météo France. This comparison is done on a collocated pixel basis and the maximum distance from the radar system evaluated is 60 km. Only one elevation angle is used in the evaluation. The quality of the algorithms is evaluated based on the normalized bias between the rain gauge and the radar retrieved rainfall accumulation (NB), the correlation (corr), and the percentage of ratio between the hourly rainfall accumulation and the rain gauge hourly accumulations between 0,8 and 1,25 (%Ratio).

To summarize, we have tested 11 algorithms:

- Two different Z-R relations with and without attenuation correction (Marshall-Palmer and the relation used by the American WSR-88D radars, i.e. $Z=200\ R^{1.6}$ and $Z=300R^{1.4}$, respectively)
- Two different R-K_{DP} relations $R=a(K_{DP}/f)^b$, from Bringi and Chandrasekar, 2001: One for the Beard and Chuang, 1987 equilibrium shape model (a=129, b=0.85) and another corresponding to the Brandes et al., 2002 equilibrium shape model (a=132, b=0.791) , with f=9.375 GHz.
- Four hybrid algorithms Z-K_{DP} : 1) Z-K_{DP1} : Marshall-Palmer (Att. corr.MP) and Beard et Chuang. 2) Z-K_{DP2} : Marshall-Palmer (Att. corr. MP) and Brandes et al. 3) Z-K_{DP3} : Fulton et al. (Att. corr WSR-88D) and Beard et Chuang. 4) Z-K_{DP4} : Fulton et al. (Att. corr. WSR-88D) and Brandes et al.
- Testud et al. (2000) ZPHI®.

4. Preliminary Results

4.1 Data set

The preliminary results presented here are obtained from both Mont Maurel and Mont Vial radars. The selected events have an average rainfall accumulation greater than 5 mm. Also, the daily average surface temperature close to the radar is high enough so that the radar beam was below the freezing level at 60 km (Figueras i Ventura et al., 2012). Table 1 lists the 15 events that satisfy the conditions above and were selected to analyze the data. All the results are stratified according to 4 thresholds on the rain gauge hourly accumulations: >0.2 mm, >1 mm, >5mm and >10 mm/h.

Table 1 Selected events and elevation angles used in the data analysis

Radar	**Elev[°]**	**Date**
Mont Vial	0.4	02, 03, 08, 29 June ; 13, 17, 19, 27 July ; 04 September ; 05, 08 November 2011
Mont Maurel	0.5	27 July ; 07 August ; 04 September ; 04 November 2011

4.2 Impact of Φ_{DP} high pass filtering and K_{DP} calculation

A moving median filter is used for filtering the noise in Φ_{DP}. In the polarimetric chain this filter is applied to the ±12 consecutive range gates (total of 25) surrounding a gate classified as PR. This corresponds to a filtering length of 6 km for Mont Maurel radar and 7,5 km for Mont Vial. If fewer than 50% of the gates in the window (i.e. 13 gates) are classified as PR, the median is not calculated. In that case, the Φ_{DP} value is obtained as a linear interpolation of the surrounding valid filtered gates. The calculation of K_{DP} is based on a linear regression over the filtered Φ_{DP} curve for 25 PR gates. As with the Φ_{DP} smoothing, K_{DP} is only valid if there are at least 13 gates classified as PR, otherwise, K_{DP} is set to 0.

In this study, we test the impact of the Φ_{DP} filter length on the rainfall retrievals. All events mentioned above were re-analysed using two shorter filter lengths (13 gates, and 7 gates), besides the initial length of 25 gates. The same tests are done

for the estimation of K_{DP} using 3 fixed filter lengths of 25, 13 and 7 gates. Fig. 1 summarizes the global results obtained by 2 distinct R-K_{DP} relations: Beard and Chuang and Brandes et al. The scatterplots show the comparison of the radar retrieved rainfall amounts for the 3 different length filters with the rainfall recorded by the rain gauges. Table 2 presents the scores for the same R-K_{DP} relationships, according to Φ_{DP} filter length (25, 13 and 7 gates).

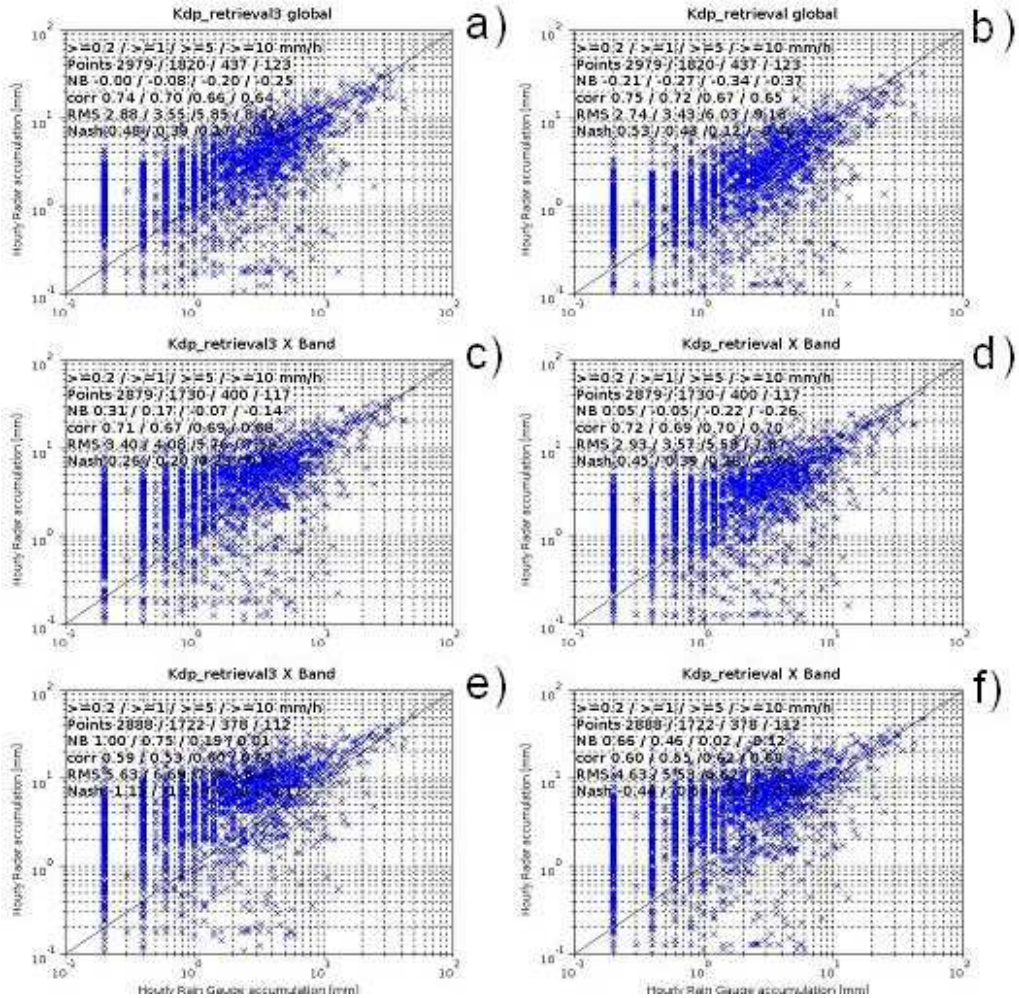

Fig. 1 global results obtained by R-K_{DP} relations (Beard and Chuang and Brandes et al.) according to different Φ_{DP} filter length: a) Brandes et al, with 25 gates c) with 13gates e) with 7 gates, b) Beard and Chong, with 25 gates, d) with 13gates, and f) with 7 gates

Table 2 R-K_{DP} results according to Φ_{DP} filter length (25, 13 and 7 gates).

R- K_{DP}	filter length	[0.2-1[				[1-5[				[5-10[				>=10			
		pts	NB	Corr	%ratio	pts	NB	Corr	%ratio	pts	NB	Corr	%ratio	pts	NB	Corr	%ratio
B-C	25	1159	0.65	0.21	6.21	1383	-0.18	0.31	21.69	314	-0.31	0.21	23.25	123	-0.37	0.65	28.46
	13	1149	1.65	0.22	4.18	1330	0.16	0.24	17.22	283	-0.19	0.20	28.27	117	-0.26	0.70	43.59
	7	1166	3.52	0.22	2.40	1344	0.97	0.20	6.47	266	0.17	0.14	21.43	112	-0.12	0.68	40.18
Brandes	25	1159	1.23	0.21	7.77	1383	0.07	0.31	17.64	314	-0.14	0.21	25.80	123	-0.25	0.64	38.21
	13	1149	2.45	0.22	4.70	1330	0.47	0.24	12.11	283	-0.00	0.20	27.56	117	-0.14	0.68	46.15
	7	1166	4.62	0.22	3.77	1344	1.39	0.20	5.65	266	0.39	0.13	15.41	112	0.01	0.67	36.61

It can be observed that NB is much higher when using the shorter filters (13 and 7 gates) for the lower precipitation classes [0.2 ,1] and [1 ,5[mm as can be expected because of the influence of phase noise which is larger for weak precipitation. For intense hourly accumulations (>=10), it can be noticed that the bias decreases significantly from –0.37 (25 gates) to –0.26 (13 gates) and to –0.12 (7 gates) for B-C R-K_{DP} algorithm and NB reduced from –0.25 (25 gates) to –0.14 (13 gates) and 0.01(7 gates) for Brandes et al. R- K_{DP} algorithm. Such improvement is even more relevant in terms of %Ratio, respectively from 28.46 to 43.59 for B-C and 38.21 to 46.15 for Brandes et al.

The results also show that, between the two distinct relations of R-K_{DP}, the Brandes et al. relation presents the best results in terms of all scores.

Table 3 Z-R relations (without and with attenuation correction) results according to Φ_{DP} filter length (25, 13 and 7 gates).

Algo	length filter	[0.2-1[				[1-5[				[5-10[				>=10			
		pts	NB	Corr	Ratio	pts	NB	Corr	Ratio	pts	NB	Corr	Ratio	pts	NB	Corr	Ratio
MP	25	1269	0.05	0.27	12.21	1525	-0.44	0.23	14.75	338	-0.65	0.16	5.92	130	-0.78	0.15	1.54
MP with att. corr	25	1269	0.21	0.26	11.66	1525	-0.24	0.27	17.97	338	-0.39	0.26	16.27	130	-0.47	0.47	15.38
	13	1268	0.24	0.25	12.54	1521	-0.22	0.27	18.15	340	-0.38	0.26	17.35	130	-0.43	0.49	19.23
	7	1267	0.26	0.24	12.55	1518	-0.20	0.26	17.72	339	-0.36	0.25	17.40	130	-0.41	0.49	20.00
WSR	25	1269	-0.07	0.24	11.11	1525	-0.47	0.21	12.39	338	-0.66	0.15	6.21	130	-0.77	0.13	2.31
WSRD with att. Corr	25	1269	0.12	0.22	10.87	1525	-0.24	0.25	16.13	338	-0.34	0.26	15.68	130	-0.37	0.45	23.08
	13	1268	0.15	0.20	11.20	1521	-0.22	0.25	15.78	340	-0.32	0.25	16.76	130	-0.32	0.47	23.85
	7	1267	0.18	0.19	11.60	1518	-0.18	0.23	15.88	339	-0.30	0.24	15.93	130	-0.29	0.47	22.31

Table 3 shows the results obtained by Z-R relations. The table shows the impact of filter length in the attenuation correction. For this kind of algorithm, the impact of the filter length is not as evident since the size of the filter impacts only the attenuation correction for Z_H. Still, it is observed that the NB slightly decreases with filter length for higher rain accumulations, while it increases for lower rain accumulations. This will be discussed in more detail in section 4.3.

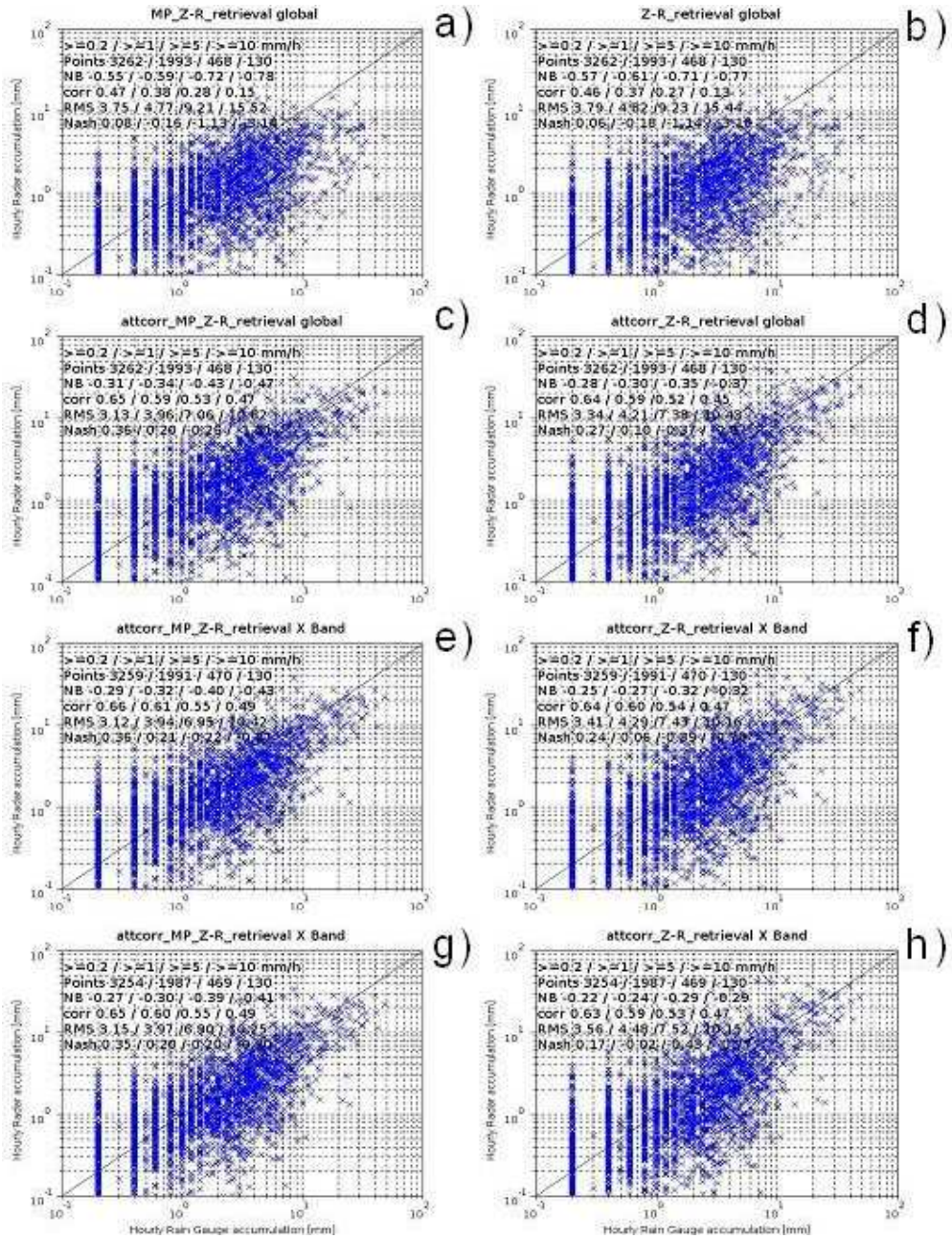

Fig. 2 QPE results: a) Marshall-Palmer relation, b) the relation used by the American WSR-88D radars] and with attenuation correction, c) Att. Corr. MP (25gates), e) (13gates), g) (7gates), d) Att. Corr. WSR-88D (25gates), f) (13gates), h) (7gates)

4.3 Impact of attenuation correction

The attenuation correction, at this stage, is performed using a simple static empirical linear relationship between the path-integrated attenuation (and differential attenuation) and Φ_{DP}. Both the specific attenuation and the specific differential attenuation are considered proportional to Φ_{DP} with a constant of proportionality (γ_H for the specific attenuation and γ_{DP} for the specific differential attenuation respectively) that is frequency dependent (Ryzhkov & Zrnic 1995). The value of γ_H was experimentally estimated using the Mont Vial radar data from scatter plots of measured Z_H versus Φ_{DP} to be 0.28. The value of γ_{DP} was deduced from ratios of γ_H/γ_{DP} mentioned in the literature (Bringi & Chandrasekar, 2001) and Snyder et al. (2010).

The impact of attenuation correction on Z-R relations is summarized in Fig. 2, which shows scatterplots of the rainfall measured by rain gauge against rainfall retrieved by 2 Z-R algorithms (Marshall-Palmer relation and the relation used by the American WSR-88D radars) with and without attenuation correction. Because the different filter lengths also impacts the attenuation correction, Fig. 2 also shows results for the 3 filter lengths: 25, 13 and 7 gates. The corresponding scores are shown in Table 3. It can be observed that, without attenuation correction, Marshall-Palmer scores are equivalent to the WSR-88D scores. For both schemes, the attenuation correction significantly improves the correlation between rain gauge and radar retrieved measurements, particularly at higher precipitation rates. There is also an improvement of the bias. Such improvement is more relevant in terms of %Ratio, respectively from 1.54 to 15.38 for MP and 2.31 to 23.08 for WSR-88D relation. It is also seen that the 7 gates length filter for Φ_{DP} performs better in terms of correlation and bias for intense hourly accumulations, but it performs poorer for weak hourly accumulations. Thus, we keep using the 25 gates length filter for the evaluation of the synthetic Z-K_{DP} algorithm. The results are presented on figure 3. It shows that the combination of attenuation corrected Marshall-Palmer and Brandes et al. performs better, both in terms of correlation and bias. We also evaluated the ZPHI algorithm and it shows best score in terms of bias but Z-K_{DP2} shows best score in terms of correlation.

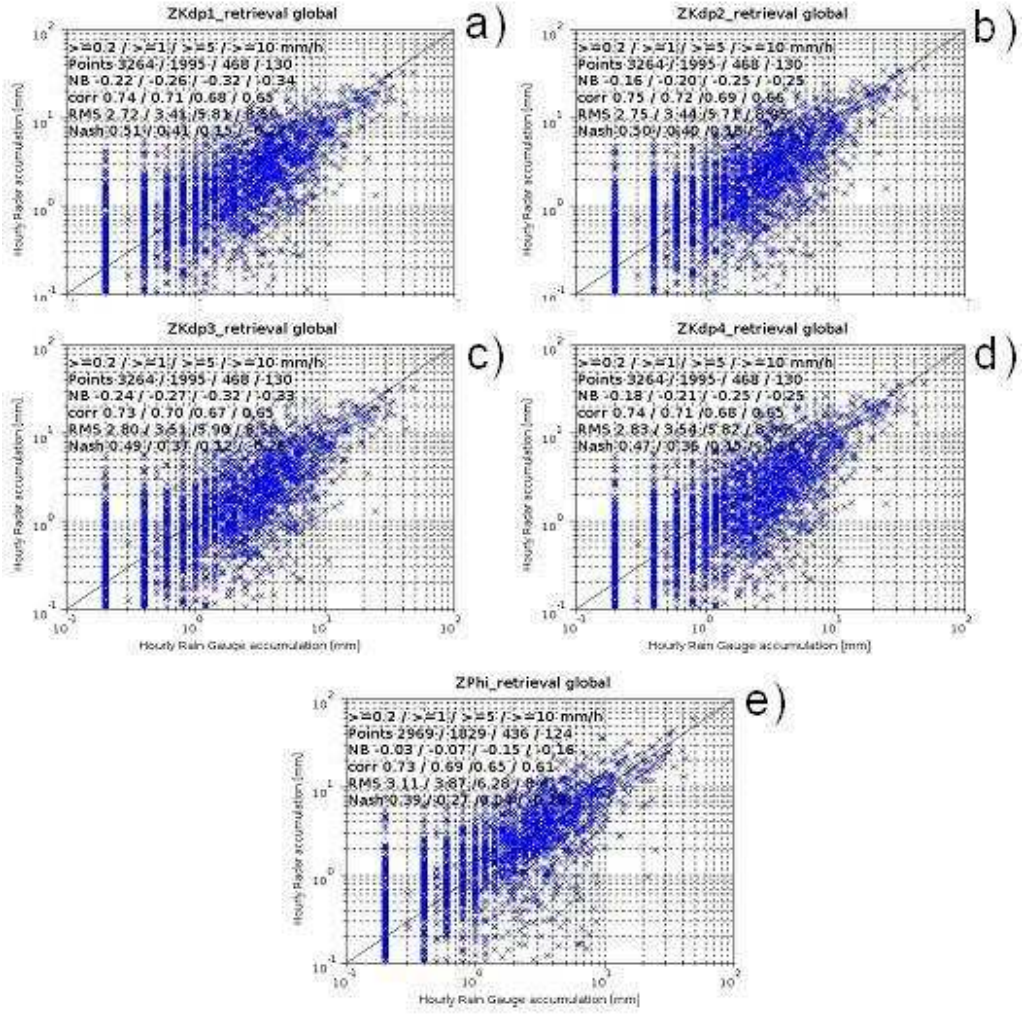

Fig. 3 QPE results : a) Z-K_{DP1}, b) Z-K_{DP2}, c) Z-K_{DP3} and d) Z-K_{DP4}

5. Conclusion

In this paper we have tested several polarimetric QPE algorithms in a single tilt configuration to determine the optimal algorithm to be implemented in the RHYTMME radar data processing chain. We have also tested the sensitivity to Φ_{DP} filter

length and K_{DP} retrieval of the various algorithms. For a fixed filter length, 25 gates seems to be a good compromise between the need to minimize the error due to phase noise and the need to estimate correctly rain cells as narrow as possible. Nevertheless the possibility to implement an adaptive filter length should be examined. Our tests show that R-K_{DP} algorithms perform better than Z-R, particularly for intensive rainfall. A hybrid Z-K_{DP} algorithm, which combines R-K_{DP} relations for intense precipitation and Z-R relations in light rain, has been tested and the one which shows the best score is Z-K_{DP2} (combination of Attenuation corrected Marshall-Palmer and Brandes et al.).

Acknowledgment

The financial support for this study was provided by the European Union, the Provence-Alpes-Côte d'Azur Region, and the French Ministry of Ecology, Energy, Sustainable Development and Sea through the RHYTMME project.

References

Boumahmoud A.-A., Fradon B., Roquain P., Perier, L., Tabary P., 2010: French operational dual-polarization chain. European Conference on Radar in Meteorology and Hydrology. ERAD2010.

Brandes EA, Ryzhkov AV, Zrnic DS., 2001: An Evaluation of Radar Rainfall Estimates from Specific Differential Phase. J. Atmos. Oceanic Technol., 18, 363-375.

Bringi V.N., Chandrasekar V., 2001: Polarimetric Doppler Weather Radar: Principles and Applications. Cambridge University Press.

Figueras i Ventura J., Boumahmoud A.-A., Fradon B., Dupuy P., Tabary P., 2012: Long-term monitoring of French polarimetric radar data quality and evaluation of several polarimetric quantitative precipitation estimators in ideal conditions for operational implementation at C-band. Quart. Jour. of the Royal Meteo. Soc., Online early release

Fulton RA, Bredienbach J.P., Seo D. J., Miller D. A., O'Bannon T., 1998: The WSR-88 rainfall algorithm. Weather Forecasting, 13, 377–395.

Marshall JS, Langille RC, Palmer WK., 1947: Measurement of rainfall by radar. J. Meteorol., 4, 186–192.

Ryzhkov, A. V., and Zrnic D. S., 1995: Precipitation and attenuation measurements at 10-cm wavelength. J. Appl. Met., 34, 2121–2134.

Snyder, J. C., Bluestein H. B., Zhang G., and Frasier S. J., 2010: Attenuation correction and hydrometeor classification of high-resolution, X-band, dual-polarized mobile radar measurements in severe convective storms. J. Atmos. Oceanic Technol., 27, 1979–2001.

Testud, J., Le Bouar E., Obligis E., and Ali-Mehenni M., 2000: The rain profiling algorithm applied to polarimetric weather radar. J. Atmos. Oceanic Technol., 17, 332-356.